Implications of computed tomography reconstruction algorithms on coronary atheroma quantification: comparison with intravascular ultrasound

Anantharaman Ramasamy [a,b], Ameer Hamid A Khan [a] Jackie Cooper [b], Judit Simon [c], Pal Maurovich-Horvat [c], Retesh Bajaj [a,b], Pieter Kitslaar [d,e], Rajiv Amersey [a], Ajay Jain [a], Andrew Deaner [a], Johan HC. Reiber [de], James C. Moon [a,f], Jouke Dijkstra [d], Patrick W. Serruys [g,h], Anthony Mathur [a,b], Andreas Baumbach [a,b], RyoTorii [i], Francesca Pugliese [a,b], Christos V.Bourantas [a,b,f,*]

[a] Department of Cardiology, Barts Heart Centre, Barts Health NHS Trust, London, UK

[b] Centre for Cardiovascular Medicine and Devices, William Harvey Research Institute, Queen Mary University London, UK

[c] MTA-SE Cardiovascular Imaging Research Group, Medical Imaging Centre, Semmelweis University, Budapest, Hungary

[d] Division of Image Processing, Department of Radiology, Leiden University Medical Center, Leiden, the Netherlands

[e] Medis Medical Imaging, Leiden, the Netherlands

[f] Institute of Cardiovascular Sciences, University College London, London, UK

[g] Faculty of Medicine, National Heart & Lung Institute, Imperial College London, UK

[h] Department of Cardiology, National University of Ireland, Galway, Ireland

[i] Department of Mechanical Engineering, University College London, London, UK

*Corresponding author. Consultant Cardiologist, Barts Heart Centre, Barts Heart Centre, West Smithfield, London EC1A 7BE. Email: cbourantas@gmail.com

Abstract

Background: Advances in coronary computed tomography angiography (CCTA) reconstruction algorithms are expected to enhance the accuracy of CCTA plaque quantification. We aim to evaluate different CCTA reconstruction approaches in assessing vessel characteristics in coronary atheroma using intravascular ultrasound (IVUS) as the reference standard.

Methods: Matched cross-sections (n=7241) from 50 vessels in 15 participants with chronic coronary syndrome who prospectively underwent CCTA and 3-vessel near-infrared spectroscopy-IVUS were included. Twelve CCTA datasets per patient were reconstructed using two different kernels, two slice thicknesses (0.75mm and 0.50mm) and three different strengths of advanced model-based iterative reconstruction (IR) algorithms. Lumen and vessel wall borders were manually annotated in every IVUS and CCTA cross-section which were co-registered using dedicated software. Image quality was sub-optimal in the reconstructions with a sharper kernel, so these were excluded. Intra-class correlation coefficient (ICC) and repeatability coefficient (RC) were used to compare the estimation of the 6 CT reconstruction approaches with those derived by IVUS.

Results: Segment-level analysis showed good agreement between CCTA and IVUS for assessing atheroma volume with approach 0.50/5 (slice thickness 0.50mm and highest strength 5 ADMIRE IR) being the best (total atheroma volume ICC: 0.91, RC: 0.67, $p<0.001$ and percentage atheroma volume ICC: 0.64, RC: 14.06, $p<0.001$). At lesion-level, there was no difference between CCTA reconstructions for detecting plaques (accuracy range: 0.64-0.67; $p=0.23$); however, approach 0.50/5 was superior in assessing IVUS-derived lesion characteristics associated with plaque vulnerability (minimum lumen area ICC: 0.64, RC: 1.31, $p<0.001$ and plaque burden ICC: 0.45, RC: 32.0, $p<0.001$).

Conclusion: CCTA reconstruction with thinner slice thickness, smooth kernel and highest strength advanced IR enabled more accurate quantification of the lumen and plaque at a segment-, and lesion-level analysis in coronary atheroma when validated against intravascular ultrasound. Clinicaltrials.gov (NCT03556644)

Keywords: Coronary computed tomography angiography; intravascular imaging; iterative reconstruction; coronary plaque quantification

Abbreviations:

ADMIRE = Advanced modeled iterative reconstruction

CCTA = Coronary computed tomography angiography

ICC = Intraclass correlation coefficient

IR = Iterative reconstruction

IVUS = Intravascular ultrasound

MLA = Minimum lumen area

NIRS = Near-infrared spectroscopy

PAV = Percentage atheroma volume

PB = Plaque burden

TAV = Total atheroma volume

Introduction

Coronary computed tomography angiography (CCTA) is an established non-invasive imaging modality to detect coronary artery disease with good diagnostic accuracy and high negative predictive value.[1, 2] CCTA has been also proposed for quantifying and characterizing coronary atherosclerotic plaques and identifying patients who are at risk of future cardiovascular events.[3-6] Despite the potential of this modality, it is today acknowledged that its efficacy in assessing plaque morphology and predicting adverse events is inferior to intravascular imaging which is regarded as the reference standard for evaluating plaque pathology.[7]

Several studies have compared CCTA against invasive imaging, and in particular intravascular ultrasound (IVUS) showing a weak but statistically significant correlation between the estimations of these two modalities.[8, 9] However, most of these studies focused on the comparison at a single cross-section and were performed using older generation CT scanners with outdated and fixed scanning parameters.[9] Newer, 3rd generation CT scanners and advanced iterative reconstruction (IR) algorithms have been developed to reduce noise, improve image quality, and provide detailed evaluation of lumen and plaque pathology. The objective of the study is to prospectively examine the efficacy of different CCTA reconstruction algorithms in identifying atherosclerotic plaques and quantifying lumen and vessel wall dimensions and plaque burden (PB) in coronary atheroma when using high-resolution IVUS imaging as the reference standard.

Methods

Studied patients

Fifteen patients who were prospectively recruited to the "Evaluation of the efficacy of computed tomographic coronary angiography in assessing coronary artery morphology and physiology" study (Clinicaltrials.gov NCT03556644) were randomly selected and included in this analysis (Figure 1). The study rationale and design have been published previously.[10] In brief, 70 patients with a chronic coronary syndrome and obstructive coronary artery disease undergoing further assessment (pressure wire or intravascular imaging) or treatment with percutaneous coronary intervention were recruited in the study. All patients underwent coronary CT angiography followed by 3-vessel near infrared

spectroscopy (NIRS)-IVUS imaging and functional assessment or treatment as per clinical indication. The study was conducted in accordance with the Declaration of Helsinki and the study protocol was approved by the local ethics committee (REC reference: 17/SC/0566). All patients provided written informed consent prior to study enrollment.

CCTA and NIRS-IVUS data acquisition

The study patients underwent CCTA using a 3rd generation dual-source CT scanner (Somatom Force, Siemens Healthineers). The scan parameters include prospective ECG-triggered sequential mode, gantry rotation time of 250ms, 2x128x0.5mm collimation with z-flying focal spot for both detectors and tube current determined by the scanner. A minimum tube voltage of 100kV was used for imaging defined by the CarekV algorithm for accurate assessment of the plaque pathology.

Prior to CCTA imaging, all patients received sublingual nitroglycerin (400mcg) and those with resting heart rate >70bpm intravenous metoprolol (up to a maximum dose of 40mg), provided there was no contraindication. A small test bolus dose of iodinated contrast material (Omnipaque 350) was used to synchronize the image acquisition start of the CT scan. This was followed by a bolus of iodinated contrast material (Omnipaque 350) of 65mls for patients with body mass index (BMI) < 25kg/m^2 or 78mls for those with BMI >25kg/m^2 which was injected intravenously at a rate of 4-5ml/s and followed by 32mls of saline chaser given at the same rate. The CT primary-dose related parameters such as CTDIvol and DLP were recorded.

Coronary angiography was performed according to the local protocol. Access site and choice of coronary equipment including guide catheters and guidewires were left to the operator's discretion. All patients received 400mcg of intracoronary nitrate prior to image acquisition. NIRS-IVUS was performed in all 3 major epicardial vessels and where possible, their major side branches with a diameter of more than 2mm using the 2.4F, high-resolution (35-65MHz) Makoto™ NIRS-IVUS Imaging System (Infraredx). The catheter was advanced approximately 5mm distal to the most distal side branch visible in coronary angiography and then pulled back at a constant speed of 0.5mm/s using an automated pullback device. The images were acquired at 30fps and digitally stored for offline analysis.

Data analysis

The collected raw CCTA data were reconstructed using 12 different reconstruction approaches that were selected following discussion with the vendor and included the reconstruction methodologies recommended for clinical use. Two different kernels, a medium smooth (b40f) and a sharper (b49f) kernel and two slice thicknesses of 0.75mm, with a 0.4mm increments, and of 0.5mm, with a 0.3mm increments, were chosen for data reconstruction. The advanced model-based IR (ADMIRE, Siemens Healthineers) was used for CCTA reconstruction whereby three adjustable strength levels were selected – ADMIRE strength 1, 2 and 5. The reconstruction approaches recommended for clinical reporting include both kernels (b40f and b49f), slice thicknesses of 0.75mm and ADMIRE 2 IR.

The reconstructed CCTA data, the coronary angiography images and the NIRS-IVUS pullbacks were reviewed, anatomical landmarks were identified and the most proximal and distal side branch that was visible in both NIRS-IVUS and CCTA were used to define the segment of interest. Stented segments were excluded from the analysis.

Quantitative coronary angiography (QCA) was performed in the segment of interest using dedicated software (QAngio XA, Medis Medical Imaging Systems, Leiden, The Netherlands). For each lesion – defined as a segment with a diameter stenosis>20%[11] – the following metrics were obtained: lesion length, reference vessel diameter (RVD), estimated using an interpolated approach, minimum lumen diameter (MLD) and diameter stenosis (DS). Tandem lesions were considered lesions with a DS>20% separated by a disease-free segment with length >5mm. In case of multiple lesions in a segment of interest the lesion with the maximum DS was used to define disease severity at a segment-level.

CCTA analysis was performed in the segment of interest blinded to NIRS-IVUS analysis using dedicated software (QAngioCT Research Edition 3.1, Medis Medical Imaging). In this segment, the lumen and vessel wall borders were extracted, and each cross-section were manually corrected by an expert analyst. The reproducibility of the expert was examined in 20 vessels against a second analyst (analysis protocol and results are shown in the supplementary file).

NIRS-IVUS segmentation was performed for the segment of interest blinded to the CCTA analysis using the QCU-CMS software (Version 4.69, Leiden, University Medical Center). The NIRS-IVUS

end-diastolic frames were retrospectively detected using a deep learning-based algorithm and in each of these frames, the lumen and external elastic membrane (EEM) borders were manually drawn.[11]

The CCTA and NIRS-IVUS images were co-registered using a dedicated in-house software (QAngioCT IVUS Matcher) developed by the Medis Medical Imaging (Figure 2). This software enables simultaneous visualization of the CCTA and NIRS-IVUS pullback and identification of corresponding cross-sections in these datasets using anatomical landmarks such as the coronary ostia and the origin of side branches that are seen in both CCTA and NIRS-IVUS. Linear interpolation is used to match images located between corresponding sections. In this way, for every annotated NIRS-IVUS frame, a corresponding CCTA cross-section is defined. This process was performed to identify matching between NIRS-IVUS and the 12 CCTA reconstruction approaches.

Comparison of CCTA and IVUS metrics

In each CCTA and NIRS-IVUS cross-section, the following metrics were obtained: lumen, vessel – or external elastic membrane (EEM) in the case of NIRS-IVUS – area, plaque area and PB. Three types of comparison were performed between CCTA and NIRS-IVUS:

- *A segment-level analysis:* For this analysis the lumen, vessel, total atheroma volume (TAV) and the percent atheroma volume (PAV) were estimated for the segment of interest in NIRS-IVUS and CCTA data and were compared.

- *A lesion-level analysis:* In NIRS-IVUS a lesion is defined as a segment with a minimum PB≥40% over three-consecutive end-diastolic frames. A lesion was considered separate from another if there was a segment of >5mm with a PB<40%.[12, 13]The same cut-off of 40% was also used to initially define a lesion in CCTA. For each lesion, its length, minimum lumen area (MLA), PB, and remodeling pattern were estimated and compared.[14]

- *A cross-sectional-level analysis:* This compared the estimations of NIRS-IVUS and CCTA for the lumen, vessel, plaque area and PB at every corresponding frame/cross-section.

Statistical analysis

Numerical values are presented as mean±standard deviation while categorical variables as absolute values and percentages. Variables were log transformed where necessary to normalize distributions and

reduce non-constant variation. Mixed effects models were used to account for clustering and to adjust for systematic bias between the different approaches. Bland-Altman, repeatability (RC) and intra-class correlation coefficient (ICC) were used to compare the agreement between NIRS-IVUS and CCTA estimations. The RC gives the interval within which 95% of test-retest measures lie with smaller values indicating better agreement. Confidence intervals for RC were obtained using bootstrap resampling.

In the segment-level analysis, the PAV and TAV were considered the most important metrics as these have been used as primary endpoints in studies examining the efficacy of novel pharmacotherapies in inhibiting atherosclerotic disease progression.[15, 16] For these, the agreement between the estimations of NIRS-IVUS and CCTA – derived by the ICC and RC were used to rank different approaches. Ranks were combined over metrics and measurement error indices using a multiplicative score function to define the best reconstruction approach. Each metric was assigned an equal weighting.

Similarly, for the lesion-level analysis the PB and MLA were considered as the most important metrics as these variables, in addition to lesion phenotype appear to define lesion vulnerability.[12, 17] The ICC and RC values between NIRS-IVUS and CCTA were computed for these two variables and used to define the best CCTA reconstruction approach for the lesion-level analysis. Finally, for the cross-sectional-level analysis, lumen, vessel, plaque area and PB were considered equally important. The agreement between CCTA and NIRS-IVUS derived by ICC and RC for these variables was used to identify the best CCTA reconstruction methodology for cross-sectional-level segmentation.

Receiver operating characteristics (ROC) curve analysis was used to examine the efficacy of different CCTA reconstruction approaches in detecting lesions identified by NIRS-IVUS and define the best PB cut-off to detect these lesions using the Youden index. This cut-off was used to repeat the lesion-level analysis and examine the agreement between NIRS-IVUS and CCTA. Statistical analysis was performed using Stata version 16 (StataCorp); a P-value<0.05 was considered statistically significant.

Results

Participant characteristics

In total 350 participants were screened, of which 70 fulfilled the criteria and were included on the study and from these 15, participants were randomly selected and included in the present analysis (Figure 1).

The baseline characteristics of the included participants are summarized in Table 1. The mean age of studied participants was 61±7 years old and the majority of participants were male (80%). Most of the participants had a family history of coronary artery disease and suffered from hypercholesterolemia. There was a balanced distribution of the studied vessels. The mean length of the studied segments on IVUS was 66.1±28.3mm and 69.9±28.5mm on CCTA. All participants were in sinus rhythm. The average heart rate during CCTA image acquisition was 61.2±8.4 bpm. In total, 7241 end-diastolic IVUS frames (50 vessels from 15 participants) were analyzed and matched with the CCTA cross-sections."

Segment-level analysis

The results of the QCA analysis at a segment-level are shown in Supplementary Table 1. Overall, 61 lesions were identified in the studied segments; 8 segments had no lesions.

Of the 12 reconstruction approaches, only those that included a smooth medium b40f kernel were included in the final analysis (Figure 3). The image quality in the 6 reconstructions with a sharper kernel (b49f) – that improves spatial resolution but considerably also increases noise – did not allow annotation of the lumen and especially, the vessel wall borders with confidence so these reconstructions were excluded from the study (Supplementary Figure 1).

The mean lumen and vessel volume, TAV and PAV were underestimated by CCTA compared with NIRS-IVUS in all approaches; however, their ICC agreement was excellent with NIRS-IVUS for the above metrics. TAV estimations with approach 0.50/5 (slice thickness 0.50mm and ADMIRE 5 IR) showed the best correlation compared with IVUS among all 6 approaches. A moderate correlation was observed for all 6 approaches for the PAV with approach 0.75/1 having the best correlation and approach 0.75/5 the smallest error among them. When combining the rankings for TAV and PAV, approach 0.50/5 provided the closest estimations to NIRS-IVUS (ICC: 0.91, RC: 0.67, $p<0.001$ and ICC: 0.64, RC: 14.06, $p<0.001$, respectively) indicating that this is the ideal method for segment-level analysis (Table 2 and Supplementary Table 2, Figure 4).

Bland-Altman analysis of TAV and PAV estimations for all 6 approaches are shown in Supplementary Figure 2. Of note, the SD of the differences between IVUS and the estimations of approach 0.50/5 was 11% smaller than the SD reported for approach 0.75/2 – that is currently recommended by the vendor in clinical practice.

Lesion-level analysis

A total of 95 lesions were detected on NIRS-IVUS imaging in 50 vessels. Of these lesions, 55 were detected by QCA; all the lesions that were not detected by QCA had a PB<60% on IVUS. In addition, QCA detected 5 lesions that were not seen by IVUS. The QCA analysis results at a lesion-level are presented in supplementary Table 1.

Two types of lesion-level analysis were performed. The first analysis used the standard NIRS-IVUS cut-off (PB≥40% over 3 consecutive end-diastolic frames) to define a lesion in CCTA. Using this cut-off, the accuracy of CCTA was moderate for detecting lesions using NIRS-IVUS as reference standard (Supplementary Table 3). CCTA underestimated lesion length and MLA but overestimated PB and remodeling index compared with NIRS-IVUS estimations (Supplementary Table 4).

ROC curve analysis was performed to define the best PB cut-off for each CCTA reconstruction approach that predicted a PB≥40% on NIRS-IVUS and this was used to identify lesions in CCTA in a repeat analysis (Figure 5). Supplementary Table 3 summarizes the accuracy of all 6 CCTA approaches using the new cut-offs. Overall, there was no difference in the performance of the 6 approaches that had a moderate overall accuracy (range: 0.64-0.67, p=0.23). The 6 CCTA approaches detected approximately two-thirds of the 95 lesions identified by IVUS (range: 63-75 lesions) with weak sensitivity but high specificity. CCTA underestimated lesion length, MLA and PB compared with IVUS (Table 3, Figure 4). Approaches 0.50/5 and 0.75/2 were both the best reconstructions in assessing the MLA (ICC:0.64, RC:1.31, p<0.001 and ICC:0.62, RC:1.42, p<0.001, respectively) and PB (ICC:0.45, RC:32.0, p<0.001 and ICC:0.53, RC:28.0, p<0.001, respectively) at a lesion-level.

Cross-sectional-level analysis

The cross-sectional-level analysis showed similar results compared to segment- and lesion-level analysis; approach 0.5/5 had the best agreement with NIRS-IVUS for assessing the lumen, vessel, plaque area and PB at a cross-sectional-level (Supplementary Table 5, Supplementary Figure 3).

Discussion

The present study evaluated the effects of different CCTA reconstruction algorithms for assessing lumen and vessel wall dimensions and quantifying plaque using NIRS-IVUS as the reference standard. We have demonstrated that 1) slice thickness and iterative reconstruction (IR) strengths influence CCTA's ability to accurately assess coronary atheroma; 2) reconstruction approach 0.50/5 with thinner slice thickness and highest IR strength has the best correlation compared with IVUS for estimating TAV and PAV in a segment-level analysis, for quantifying the MLA and PB at a lesion-level and for assessing lumen, vessel wall and plaque area and PB at a cross-sectional-level.

Advances in CCTA acquisition and the development of efficient post-processing methodologies have improved image resolution and reduced radiation dose enabling its broad use in clinical practice to detect coronary artery disease. Several studies in recent years have investigated and highlighted the importance of the reconstruction parameters in CCTA volumetric analyses. Puchner et al. demonstrated that iterative CT angiography reconstruction is superior to filter back-projection and adaptive statistical modelling in quantifying PB;[18] Achenbach et al. showed that slice thickness and reconstruction kernels influence the attenuation of non-calcified plaques,[19] while Qian et al. highlighted the role of slice thickness on the quantification of calcific burden.[20] Finally, Motoyama et al compared ultra-high-resolution CT angiography (slice thickness = 0.25mm) with conventional CCT angiography (slice thickness = 0.50mm) and showed that high-resolution CT angiography had an improved diagnostic accuracy for detecting >50% stenosis against coronary angiography (AUC 0.98 vs 0.80).[21] However the optimal reconstruction approach in 3rd generation CT scanners have not been previously well established in the literature. However, the optimal reconstruction approach in 3rd generation CT scanners have not been examined in the current literature.

Our study was designed to address this unmet need and identify the optimal reconstruction parameters for future CCTA studies of atherosclerosis.[10] Its prospective design allowed us to pay attention to the fine details. Data acquisition was optimal and CCTA imaging was performed in all patients with a minimum tube voltage of 100kV (13 participants had CCTA with 100kV and the remaining two participants with 110kV and 120kV due to their increased body weight) as this can affect plaque attenuation and, potentially, PB quantification.[22] In contrast to previous studies, that included patients who had IVUS for clinical reasons in a single vessel to assess disease severity or to guide

revascularization,[23-25] our analysis included prospective study participants with established obstructive coronary artery disease that underwent 3-vessel NIRS-IVUS imaging in all the epicardial coronary arteries and their major sides branches irrespective of the presence of coronary artery disease in these segments. Moreover, it implemented a robust validation methodology to evaluate the performance of CT angiography at a segment, lesion, and cross-sectional level and in contrast to previous reports, it introduced IVUS-specific criteria to define lesions.[24, 26] Finally, the present study used a dedicated software to identify matching between NIRS-IVUS and CCTA data and included all lesions and frames within the segments of interest for the lesion and cross-sectional level analysis, respectively. Therefore, this analysis overcome the bias introduced by other studies that focused on the comparison of the two modalities in the most diseased lesion,[24] at the MLA,[23] or selected cross-sections,[25] and enabled more thorough evaluation of the performance of CCTA and its limitations in assessing lumen and vessel wall dimensions and PB (Supplementary Figure 4).

We found that a combination of a medium smooth kernel, a thinner slice thickness and an increased strength IR reconstruction, that is not currently recommended by the vendor for clinical use, provides closer estimations to NIRS-IVUS compared with the other reconstruction approaches. This finding contradicts a previous study that showed a superior image quality using the medium strength older-SAFIRE 3 IR.[27] In that study, a higher strength IR resulted in a plastic like appearance of the lumen but had overall superior signal-to-noise and contrast-to-noise ratio than the other reconstruction algorithms. These features appear to allow advanced ADMIRE IR to better delineate anatomical borders and edges and in combination with a thinner slice thickness to enable more accurate assessment of lumen and vessel wall dimensions.[28] Therefore, this approach should be preferred in serial CCTA studies to assess the effect of novel pharmacotherapies on plaque evolution. In addition, this approach should be preferred for training artificial intelligence-based algorithms that will rely on the annotations of the expert analyst to fast and accurately segment CCTA imaging data.[29] Given the fact that MLA and PB are predictors of plaque vulnerability,[30-32] we postulate that the use of the 0.5/5 reconstruction approach will allow more accurate detection of high-risk lesions and patients.

Our study had several limitations. 1) We evaluated CCTA reconstruction algorithm from a single vendor, thus it is unclear whether these findings can be generalized to other CCTA systems. However,

we believe that this study is important as it underscores for the first time, the need to perform similar studies in different scanners and identify the optimal reconstruction methodology for each vendor, as optimal data reconstruction is likely to enable more accurate detection of high-risk lesions and precise assessment of the effects of novel pharmacotherapies on atheroma burden. 2) The number of the studied participants and segments were relatively small; however, the analysis of a larger numbers of segments using 12 different reconstruction approaches would have been challenging as CCTA segmentation was performed manually at every cross-section. 3) We did not assess the effects of different reconstruction algorithms on plaque composition and on the identification of plaque features associated with increased vulnerability such as napkin ring sign, calcific spots and attenuated plaques. However, atheroma burden is the most important predictor of cardiovascular events in imaging studies of atherosclerosis and the most established surrogate endpoint of assessing the implications of novel therapies on plaque evolution.[12, 33, 34] Besides, the accurate delineation of plaque region is the first step for assessing its composition and morphological characteristics either by visual inspection or by performing radiomic analysis.[35] 4) Although approach 0.50/5 was consistently superior to the other reconstruction methods in assessing lumen and plaque dimensions, it unclear if this is clinically relevant in the context of the relative large inter- and intra-observer variability of CCTA.[36] However, this limitation is likely to be overcome in the future with the development of advanced methodologies for the fully automated segmentation of CCTA data. 5) The patients included in the present study had extensive coronary artery disease and increased PB; therefore, it is unclear whether the findings of our analysis are applicable to patients with less advanced atherosclerosis.

In conclusion, CCTA reconstruction with medium smooth kernel, thinner slice thickness and highest strength IR enabled accurate volumetric analyses at a segment-level and lesion-specific variable estimations in coronary atheroma when validated against NIRS-IVUS. Future CCTA studies evaluating the effects of novel pharmacotherapies on atheroma burden and detection of high-risk lesions may adopt this approach for accurate CCTA segmentation.

Table 1. Baseline demographics of the studied patients.

	(n=15)
Age (years)	61±7
Gender (male)	12 (80%)
Smoking history	6 (40%)
Family history of CAD	11 (73%)
Previous acute coronary syndrome	1 (7%)
Previous cerebrovascular event	1 (7%)
Co-morbidities	
Diabetes mellitus	3 (20%)
Hypertension	5 (33%)
Hypercholesterolemia	10 (67%)
Renal failure*	0 (0%)
Previous PCI	1 (7%)
LV function**	
Normal LV function	14 (93%)
Impaired LV function	1 (7%)
Studied vessels	**(n=50)**
Left anterior descending artery	16 (32%)
Left circumflex artery	13 (26%)
Right coronary artery	15 (30%)
Intermediate ramus branch	1 (2%)
Diagonal branch	1 (2%)
Obtuse marginal branch	4 (8%)

Table footnote: CAD, coronary artery disease; LV, left ventricle; PCI, percutaneous coronary intervention.

*Renal failure is defined as an estimated glomerular filtration rate of <60ml/min/1.73m^2** Impaired LV function is defined as LV ejection fraction <50%.

Table 2. Comparison of TAV and PAV estimations between NIRS-IVUS and CCTA reconstruction approaches at a segment-level.

NIRS-IVUS and CT reconstructions	Absolute estimations	Mean±SD of differences	ICC	P	RC	P	Overall rank*
TAV (mm^3)							
NIRS-IVUS	409.2±265.4						
CCTA Approach 0.75/1	177.6±112.5	231.6±189.4	0.89 (0.82-0.94)	<0.001	0.70 (0.59-0.82)	<0.001	4
CCTA Approach 0.75/2	178.7±123.6	230.4±191.3	0.88 (0.80-0.93)	<0.001	0.76 (0.65-0.88)	<0.001	6
CCTA Approach 0.75/5	142.1±96.5	267.1±199.9	0.90 (0.82-0.94)	<0.001	0.69 (0.55-0.82)	<0.001	3
CCTA Approach 0.50/1	190.7±136.5	218.5±170.2	0.90 (0.84-0.95)	<0.001	0.68 (0.56-0.80)	<0.001	2
CCTA Approach 0.50/2	176.7±121.4	232.5±180.8	0.88 (0.80-0.93)	<0.001	0.75 (0.61-0.89)	<0.001	5
CCTA Approach 0.50/5	155.5±114.5	253.6±177.9	0.91 (0.84-0.95)	<0.001	0.67 (0.52-0.83)	<0.001	1
PAV (%)							
NIRS-IVUS	43.40±8.13						
CCTA Approach 0.75/1	29.54±9.85	13.86±7.31	0.67 (0.49-0.80)	<0.001	14.32 (12.06-16.59)	<0.001	2
CCTA Approach 0.75/2	28.47±9.35	14.93±7.53	0.63 (0.43-0.77)	<0.001	14.77 (12.74-16.80)	<0.001	4

CCTA Approach 0.75/5	25.65±8.92	17.75±7.14	0.65 (0.46-0.79)	<0.001	13.98 (11.46-16.51)	<0.001
CCTA Approach 0.50/1	30.26±9.25	13.14±7.62	0.62 (0.41-0.76)	<0.001	14.93 (12.30-17.56)	<0.001
CCTA Approach 0.50/2	29.46±9.07	13.94±7.74	0.61 (0.40-0.76)	<0.001	14.98 (12.60-17.35)	<0.001
CCTA Approach 0.50/5	26.30±8.82	17.10±7.18	0.64 (0.45-0.78)	<0.001	14.06 (11.20-16.92)	<0.001

Table footnote: ICC, intraclass correlation; PAV, percent atheroma volume; RC, repeatability coefficient; TAV, total atheroma volume.

Note: Numbers in parentheses are 95% CIs.

*The rank is based on the combination of ICC and RC which were used to compare IVUS and CCTA algorithms. Lower rank indicates a better accuracy against IVUS estimations (rank 1 = best and rank 5 = worst)

Table 3. Accuracy of CCTA reconstruction algorithms for assessing lesion characteristics.

NIRS-IVUS and CT reconstructions	Absolute estimations	Mean±SD of differences	ICC	P	RC	P	Overall Rank*
Lesion length (mm)							
NIRS-IVUS	21.05±18.71						
CCTA Approach 0.75/1	22.40±17.17	0.41±19.49	0.41 (0.25-0.60)	<0.001	38.2 (32.1-44.4)	<0.001	5
CCTA Approach 0.75/2	16.86±14.95	5.90±12.59	0.73 (0.61-0.83)	<0.001	24.7 (18.8-30.6)	<0.001	1
CCTA Approach 0.75/5	16.69±15.90	6.05±17.46	0.51 (0.34-0.67)	<0.001	34.2 (26.6-41.8)	<0.001	4
CCTA Approach 0.50/1	20.54±17.53	1.80±16.96	0.56 (0.41-0.70)	<0.001	33.2 (26.7-39.7)	<0.001	2
CCTA Approach 0.50/2	15.86±13.19	6.12±16.76	0.48 (0.32-0.65)	<0.001	32.9 (26.5-39.2)	<0.001	3
CCTA Approach 0.50/5	16.19±18.43	6.41±19.89	0.43 (0.27-0.61)	<0.001	39.0 (30.6-47.3)	<0.001	6
MLA (mm^2)							
NIRS-IVUS	4.84±3.25						
CCTA Approach 0.75/1	3.18±2.00	1.22±2.05	0.64 (0.49-0.76)	<0.001	1.22 (1.00-1.45)	<0.001	1
CCTA Approach 0.75/2	3.83±3.16	0.70±2.44	0.62 (0.46-0.75)	<0.001	1.42 (0.82-2.02)	<0.001	2

CCTA Approach 0.75/5	3.23±2.19	1.08±2.25	0.54 (0.38-0.70)	<0.001	1.59 (1.13-2.04)	<0.001	4
CCTA Approach 0.50/1	2.87±1.89	1.72±2.53	0.54 (0.38-0.70)	<0.001	1.44 (1.02-1.86)	<0.001	5
CCTA Approach 0.50/2	2.95±2.04	1.84±2.80	0.65 (0.40-0.70)	<0.001	1.35 (0.97-1.74)	<0.001	5
CCTA Approach 0.50/5	3.45±2.75	1.23±2.42	0.64 (0.49-0.76)	<0.001	1.31 (0.94-1.67)	<0.001	2
PB (%)							
NIRS-IVUS	63.0±13.0						
CCTA Approach 0.75/1	60.1±19.8	4.20±18.58	0.38 (0.20-0.56)	<0.001	36.4 (30.7-42.1)	<0.001	5
CCTA Approach 0.75/2	60.7±17.0	5.14±14.26	0.53 (0.37-0.70)	<0.001	28.0 (23.4-32.5)	<0.001	1
CCTA Approach 0.75/5	56.0±21.9	9.48±17.53	0.47 (0.32-0.61)	<0.001	34.4 (30.2-38.6)	<0.001	3
CCTA Approach 0.50/1	63.7±17.9	0.33±18.13	0.33 (0.14-0.53)	<0.001	35.5 (30.8-40.2)	<0.001	5
CCTA Approach 0.50/2	64.0±16.6	-0.14±16.36	0.41 (0.22-0.60)	<0.001	32.1 (27.5-36.6)	<0.001	4
CCTA Approach 0.50/5	57.2±18.7	7.26±16.32	0.45 (0.29-0.61)	<0.001	32.0 (28.0-35.9)	<0.001	2
Remodeling Index							
NIRS-IVUS	0.84±0.22						
CCTA Approach 0.75/1	0.70±0.46	-0.06±0.32	0.37 (0.09-0.60)	0.005	0.63 (0.44-0.83)	<0.001	4
CCTA Approach 0.75/2	0.79±0.41	-0.12±0.30	0.44 (0.18-0.65)	<0.001	0.58 (0.43-0.73)	<0.001	1
CCTA Approach 0.75/5	0.79±0.41	-0.08±0.37	0.14 (0.00-0.41)	0.17	0.73 (0.54-0.91)	<0.001	6

CCTA Approach 0.50/1	0.72±0.45	-0.09±0.30	0.37 (0.11-0.58)	0.004	0.58 (0.40-0.75)	<0.001	2
CCTA Approach 0.50/2	0.81±0.39	-0.12±0.32	0.37 (0.11-0.58)	0.003	0.63 (0.49-0.76)	<0.001	3
CCTA Approach 0.50/5	0.93±0.44	-0.13±0.42	0.38 (0.12-0.59)	0.003	0.81 (0.54-1.09)	<0.001	5

Table footnote: ICC, intra-class correlation; MLA, minimum lumen area; PB, plaque burden; SD, standard deviation; RC, repeatability coefficient.

Note: Numbers in parentheses are 95% CIs.

*The rank is based on the combination of ICC and RC which were used to compare IVUS and CCTA algorithms. Lower rank indicates a better accuracy against IVUS estimations (rank 1 = best and rank 5 = worst).

SUPPLEMENTARY MATERIALS

Reproducibility analysis

Twenty randomly chosen vessels were included in the reproducibility analysis. An expert analyst with 5 years of cardiac CT imaging expertise manually segmented these vessels and annotated the lumen and vessel wall borders twice within a 2-month interval and their estimations were compared to examine the intra-observer variability. The inter-observer variability was tested in the same dataset using the estimations of a second analyst with 6 years' experience in cardiac CT analysis from Corelab (MTA-SE Cardiovascular Imaging Research Group, Hungary) with established reproducibility. The agreement of the annotations was tested using ICC. The results of the reproducibility analysis are presented in the Supplementary Table 6 and are consistent with those reported in the literature.

The reproducibility of the NIRS-IVUS analysis has been presented in a recent publication.[37]

References

1. Miller JM, Rochitte CE, Dewey M, Arbab-Zadeh A, Niinuma H, Gottlieb I, Paul N, Clouse ME, Shapiro EP, Hoe J, Lardo AC, Bush DE, de Roos A, Cox C, Brinker J and Lima JA. Diagnostic performance of coronary angiography by 64-row CT. *N Engl J Med*. 2008;359:2324-36.
2. Budoff MJ, Dowe D, Jollis JG, Gitter M, Sutherland J, Halamert E, Scherer M, Bellinger R, Martin A, Benton R, Delago A and Min JK. Diagnostic performance of 64-multidetector row coronary computed tomographic angiography for evaluation of coronary artery stenosis in individuals without known coronary artery disease: results from the prospective multicenter ACCURACY (Assessment by Coronary Computed Tomographic Angiography of Individuals Undergoing Invasive Coronary Angiography) trial. *J Am Coll Cardiol*. 2008;52:1724-32.
3. Ferencik M, Mayrhofer T, Bittner DO, Emami H, Puchner SB, Lu MT, Meyersohn NM, Ivanov AV, Adami EC, Patel MR, Mark DB, Udelson JE, Lee KL, Douglas PS and Hoffmann U. Use of High-Risk Coronary Atherosclerotic Plaque Detection for Risk Stratification of Patients With Stable Chest Pain: A Secondary Analysis of the PROMISE Randomized Clinical Trial. *JAMA Cardiol*. 2018;3:144-152.
4. Maurovich-Horvat P, Schlett CL, Alkadhi H, Nakano M, Otsuka F, Stolzmann P, Scheffel H, Ferencik M, Kriegel MF, Seifarth H, Virmani R and Hoffmann U. The napkin-ring sign indicates advanced atherosclerotic lesions in coronary CT angiography. *JACC Cardiovasc Imaging*. 2012;5:1243-52.
5. Motoyama S, Sarai M, Harigaya H, Anno H, Inoue K, Hara T, Naruse H, Ishii J, Hishida H, Wong ND, Virmani R, Kondo T, Ozaki Y and Narula J. Computed tomographic angiography characteristics of atherosclerotic plaques subsequently resulting in acute coronary syndrome. *J Am Coll Cardiol*. 2009;54:49-57.
6. Puchner SB, Liu T, Mayrhofer T, Truong QA, Lee H, Fleg JL, Nagurney JT, Udelson JE, Hoffmann U and Ferencik M. High-risk plaque detected on coronary CT angiography predicts acute coronary syndromes independent of significant stenosis in acute chest pain: results from the ROMICAT-II trial. *J Am Coll Cardiol*. 2014;64:684-92.
7. Johnson TW, Räber L, di Mario C, Bourantas C, Jia H, Mattesini A, Gonzalo N, de la Torre Hernandez JM, Prati F, Koskinas K, Joner M, Radu MD, Erlinge D, Regar E, Kunadian V, Maehara A, Byrne RA, Capodanno D, Akasaka T, Wijns W, Mintz GS and Guagliumi G. Clinical use of intracoronary imaging. Part 2: acute coronary syndromes, ambiguous coronary angiography findings, and guiding interventional decision-making: an expert consensus document of the European Association of Percutaneous Cardiovascular Interventions. *Eur Heart J*. 2019;40:2566-2584.
8. Voros S, Rinehart S, Qian Z, Joshi P, Vazquez G, Fischer C, Belur P, Hulten E and Villines TC. Coronary atherosclerosis imaging by coronary CT angiography: current status, correlation with intravascular interrogation and meta-analysis. *JACC Cardiovasc Imaging*. 2011;4:537-48.
9. Fischer C, Hulten E, Belur P, Smith R, Voros S and Villines TC. Coronary CT angiography versus intravascular ultrasound for estimation of coronary stenosis and atherosclerotic plaque burden: a meta-analysis. *J Cardiovasc Comput Tomogr*. 2013;7:256-66.
10. Ramasamy A, Safi H, Moon JC, Andiapen M, Rathod KS, Maurovich-Horvat P, Bajaj R, Serruys PW, Mathur A, Baumbach A, Pugliese F, Torii R and Bourantas CV. Evaluation of the Efficacy of Computed Tomographic Coronary Angiography in Assessing Coronary Artery Morphology and Physiology: Rationale and Study Design. *Cardiology*. 2020;145:285-293.
11. Mintz GS, Garcia-Garcia HM, Nicholls SJ, Weissman NJ, Bruining N, Crowe T, Tardif JC and Serruys PW. Clinical expert consensus document on standards for acquisition, measurement and reporting of intravascular ultrasound regression/progression studies.

EuroIntervention : journal of EuroPCR in collaboration with the Working Group on Interventional Cardiology of the European Society of Cardiology. 2011;6:1123-30, 9.
12. Stone GW, Maehara A, Lansky AJ, de Bruyne B, Cristea E, Mintz GS, Mehran R, McPherson J, Farhat N, Marso SP, Parise H, Templin B, White R, Zhang Z and Serruys PW. A prospective natural-history study of coronary atherosclerosis. *N Engl J Med*. 2011;364:226-35.
13. Garcia-Garcia HM, Gomez-Lara J, Gonzalo N, Garg S, Shin ES, Goedhart D and Serruys PW. A comparison of the distribution of necrotic core in bifurcation and non-bifurcation coronary lesions: an in vivo assessment using intravascular ultrasound radiofrequency data analysis. *EuroIntervention : journal of EuroPCR in collaboration with the Working Group on Interventional Cardiology of the European Society of Cardiology*. 2010;6:321-7.
14. Bourantas CV, Räber L, Sakellarios A, Ueki Y, Zanchin T, Koskinas KC, Yamaji K, Taniwaki M, Heg D, Radu MD, Papafaklis MI, Kalatzis F, Naka KK, Fotiadis DI, Mathur A, Serruys PW, Michalis LK, Garcia-Garcia HM, Karagiannis A and Windecker S. Utility of Multimodality Intravascular Imaging and the Local Hemodynamic Forces to Predict Atherosclerotic Disease Progression. *JACC: Cardiovascular Imaging*. 2020;13:1021-1032.
15. Nicholls SJ, Ballantyne CM, Barter PJ, Chapman MJ, Erbel RM, Libby P, Raichlen JS, Uno K, Borgman M, Wolski K and Nissen SE. Effect of Two Intensive Statin Regimens on Progression of Coronary Disease. *New England Journal of Medicine*. 2011;365:2078-2087.
16. Nicholls SJ, Puri R, Anderson T, Ballantyne CM, Cho L, Kastelein JJP, Koenig W, Somaratne R, Kassahun H, Yang J, Wasserman SM, Scott R, Ungi I, Podolec J, Ophuis AO, Cornel JH, Borgman M, Brennan DM and Nissen SE. Effect of Evolocumab on Progression of Coronary Disease in Statin-Treated Patients: The GLAGOV Randomized Clinical Trial. *JAMA*. 2016;316:2373-2384.
17. Erlinge D, Maehara A, Ben-Yehuda O, Bøtker HE, Maeng M, Kjøller-Hansen L, Engstrøm T, Matsumura M, Crowley A, Dressler O, Mintz GS, Fröbert O, Persson J, Wiseth R, Larsen AI, Okkels Jensen L, Nordrehaug JE, Bleie Ø, Omerovic E, Held C, James SK, Ali ZA, Muller JE and Stone GW. Identification of vulnerable plaques and patients by intracoronary near-infrared spectroscopy and ultrasound (PROSPECT II): a prospective natural history study. *Lancet*. 2021;397:985-995.
18. Puchner SB, Ferencik M, Maehara A, Stolzmann P, Ma S, Do S, Kauczor HU, Mintz GS, Hoffmann U and Schlett CL. Iterative Image Reconstruction Improves the Accuracy of Automated Plaque Burden Assessment in Coronary CT Angiography: A Comparison With Intravascular Ultrasound. *AJR Am J Roentgenol*. 2017;208:777-784.
19. Achenbach S, Boehmer K, Pflederer T, Ropers D, Seltmann M, Lell M, Anders K, Kuettner A, Uder M, Daniel WG and Marwan M. Influence of slice thickness and reconstruction kernel on the computed tomographic attenuation of coronary atherosclerotic plaque. *J Cardiovasc Comput Tomogr*. 2010;4:110-5.
20. Qian Z, Dhungel A, Vazquez G, Weeks M, Voros S and Rinehart S. Coronary artery calcium: 0.5 mm slice-thickness reconstruction with adjusted attenuation threshold outperforms 3.0 mm by validating against spatially registered intravascular ultrasound with radiofrequency backscatter. *Acad Radiol*. 2015;22:1128-37.
21. Motoyama S, Ito H, Sarai M, Nagahara Y, Miyajima K, Matsumoto R, Doi Y, Kataoka Y, Takahashi H, Ozaki Y, Toyama H and Katada K. Ultra-High-Resolution Computed Tomography Angiography for Assessment of Coronary Artery Stenosis. *Circ J*. 2018;82:1844-1851.
22. Matsumoto Y, Muraoka Y, Funama Y, Mito S, Masuda T, Sato T, Akita T and Awai K. Analysis of the anatomical features of pulmonary veins on pre-procedural cardiac CT

images resulting in incomplete cryoballoon ablation for atrial fibrillation. *J Cardiovasc Comput Tomogr*. 2019;13:118-127.
23. Voros S, Rinehart S, Qian Z, Vazquez G, Anderson H, Murrieta L, Wilmer C, Carlson H, Taylor K, Ballard W, Karmpaliotis D, Kalynych A and Brown C, 3rd. Prospective validation of standardized, 3-dimensional, quantitative coronary computed tomographic plaque measurements using radiofrequency backscatter intravascular ultrasound as reference standard in intermediate coronary arterial lesions: results from the ATLANTA (assessment of tissue characteristics, lesion morphology, and hemodynamics by angiography with fractional flow reserve, intravascular ultrasound and virtual histology, and noninvasive computed tomography in atherosclerotic plaques) I study. *JACC Cardiovascular interventions*. 2011;4:198-208.
24. Conte E, Mushtaq S, Pontone G, Li Piani L, Ravagnani P, Galli S, Collet C, Sonck J, Di Odoardo L, Guglielmo M, Baggiano A, Trabattoni D, Annoni A, Mancini ME, Formenti A, Muscogiuri G, Magatelli M, Nicoli F, Poggi C, Fiorentini C, Bartorelli AL, Pepi M, Montorsi P and Andreini D. Plaque quantification by coronary computed tomography angiography using intravascular ultrasound as a reference standard: a comparison between standard and last generation computed tomography scanners. *Eur Heart J Cardiovasc Imaging*. 2020;21:191-201.
25. Kruk M, Wardziak Ł, Mintz GS, Achenbach S, Pręgowski J, Rużyłło W, Dzielińska Z, Demkow M, Witkowski A and Kępka C. Accuracy of coronary computed tomography angiography vs intravascular ultrasound for evaluation of vessel area. *J Cardiovasc Comput Tomogr*. 2014;8:141-8.
26. Boogers MJ, Broersen A, van Velzen JE, de Graaf FR, El-Naggar HM, Kitslaar PH, Dijkstra J, Delgado V, Boersma E, de Roos A, Schuijf JD, Schalij MJ, Reiber JH, Bax JJ and Jukema JW. Automated quantification of coronary plaque with computed tomography: comparison with intravascular ultrasound using a dedicated registration algorithm for fusion-based quantification. *Eur Heart J*. 2012;33:1007-16.
27. Wang R, Schoepf UJ, Wu R, Nance JW, Jr., Lv B, Yang H, Li F, Lu D and Zhang Z. Diagnostic accuracy of coronary CT angiography: comparison of filtered back projection and iterative reconstruction with different strengths. *J Comput Assist Tomogr*. 2014;38:179-84.
28. Thomas Flohr BS and Juergen Merz PA. SOMATOM FORCE The New Class in CT. 2016.
29. Lin A, Manral N, McElhinney P, Killekar A, Matsumoto H, Kwiecinski J, Pieszko K, Razipour A, Grodecki K, Park C, Otaki Y, Doris M, Kwan AC, Han D, Kuronuma K, Flores Tomasino G, Tzolos E, Shanbhag A, Goeller M, Marwan M, Gransar H, Tamarappoo BK, Cadet S, Achenbach S, Nicholls SJ, Wong DT, Berman DS, Dweck M, Newby DE, Williams MC, Slomka PJ and Dey D. Deep learning-enabled coronary CT angiography for plaque and stenosis quantification and cardiac risk prediction: an international multicentre study. *Lancet Digit Health*. 2022;4:e256-e265.
30. Nadjiri J, Hausleiter J, Jähnichen C, Will A, Hendrich E, Martinoff S and Hadamitzky M. Incremental prognostic value of quantitative plaque assessment in coronary CT angiography during 5 years of follow up. *J Cardiovasc Comput Tomogr*. 2016;10:97-104.
31. Motoyama S, Ito H, Sarai M, Kondo T, Kawai H, Nagahara Y, Harigaya H, Kan S, Anno H, Takahashi H, Naruse H, Ishii J, Hecht H, Shaw LJ, Ozaki Y and Narula J. Plaque Characterization by Coronary Computed Tomography Angiography and the Likelihood of Acute Coronary Events in Mid-Term Follow-Up. *J Am Coll Cardiol*. 2015;66:337-46.
32. Williams MC, Kwiecinski J, Doris M, McElhinney P, D'Souza MS, Cadet S, Adamson PD, Moss AJ, Alam S, Hunter A, Shah ASV, Mills NL, Pawade T, Wang C, Weir McCall J, Bonnici-Mallia M, Murrills C, Roditi G, van Beek EJR, Shaw LJ, Nicol ED, Berman DS, Slomka PJ, Newby DE, Dweck MR and Dey D. Low-Attenuation Noncalcified Plaque on Coronary Computed Tomography Angiography Predicts Myocardial Infarction: Results From

the Multicenter SCOT-HEART Trial (Scottish Computed Tomography of the HEART). *Circulation*. 2020;141:1452-1462.
33. Lee SE, Sung JM, Rizvi A, Lin FY, Kumar A, Hadamitzky M, Kim YJ, Conte E, Andreini D, Pontone G, Budoff MJ, Gottlieb I, Lee BK, Chun EJ, Cademartiri F, Maffei E, Marques H, Leipsic JA, Shin S, Hyun Choi J, Chinnaiyan K, Raff G, Virmani R, Samady H, Stone PH, Berman DS, Narula J, Shaw LJ, Bax JJ, Min JK and Chang HJ. Quantification of Coronary Atherosclerosis in the Assessment of Coronary Artery Disease. *Circ Cardiovasc Imaging*. 2018;11:e007562.
34. Tufaro V, Serruys PW, Räber L, Bennett MR, Torii R, Gu SZ, Onuma Y, Mathur A, Baumbach A and Bourantas C. Intravascular imaging assessment of pharmacotherapies targeting atherosclerosis: advantages and limitations in predicting their prognostic implications. *Cardiovasc Res*. 2022.
35. Kolossváry M, Park J, Bang JI, Zhang J, Lee JM, Paeng JC, Merkely B, Narula J, Kubo T, Akasaka T, Koo BK and Maurovich-Horvat P. Identification of invasive and radionuclide imaging markers of coronary plaque vulnerability using radiomic analysis of coronary computed tomography angiography. *Eur Heart J Cardiovasc Imaging*. 2019;20:1250-1258.
36. Symons R, Morris JZ, Wu CO, Pourmorteza A, Ahlman MA, Lima JA, Chen MY, Mallek M, Sandfort V and Bluemke DA. Coronary CT Angiography: Variability of CT Scanners and Readers in Measurement of Plaque Volume. *Radiology*. 2016;281:737-748.
37. Bajaj R, Huang X, Kilic Y, Ramasamy A, Jain A, Ozkor M, Tufaro V, Safi H, Erdogan E, Serruys PW, Moon J, Pugliese F, Mathur A, Torii R, Baumbach A, Dijkstra J, Zhang Q and Bourantas CV. Advanced deep learning methodology for accurate, real-time segmentation of high-resolution intravascular ultrasound images. *Int J Cardiol*. 2021.

Supplementary Table 1. QCA analysis at a segment- and lesion level.

	Segment level analysis (n=42)	Lesion level analysis (n=61)
Lesion length (mm)	13.3 ± 9.2	12.0 ± 8.3
Reference lumen diameter (mm)	2.9 ± 0.7	2.9 ± 0.7
Minimum lumen diameter (mm)	1.8 ± 0.7	1.9 ± 0.6
Diameter stenosis (%)	37.4 ± 13.4	35.5 ± 12.3

Supplementary Table 2. Comparison of lumen and vessel wall volume estimations between IVUS and CCTA reconstruction approaches at a segment-level.

NIRS-IVUS and CT Reconstructions	Absolute estimations	Mean ± SD of differences	ICC	P	RC	P	Overall Rank*
Lumen volume (mm^3)							
NIRS-IVUS	554.6 ± 439.9						
CCTA Approach 0.75/1	437.2 ± 329.7	117.4 ± 127.3	0.98 (0.97-0.99)	<0.001	0.289 (0.228-0.350)	<0.001	4
CCTA Approach 0.75/2	442.8 ± 314.9	111.8 ± 148.3	0.99 (0.97-0.99)	<0.001	0.251 (0.192-0.310)	<0.001	3
CCTA Approach 0.75/5	419.4 ± 308.8	135.2 ± 142.1	0.99 (0.98-0.99)	<0.001	0.229 (0.152-0.307)	<0.001	1
CCTA Approach 0.50/1	423.0 ± 290.1	131.6 ± 178.6	0.98 (0.96-0.99)	<0.001	0.296 (0.224-0.368)	<0.001	5
CCTA Approach 0.50/2	414.8 ± 292.2	139.8 ± 177.1	0.97 (0.94-0.98)	<0.001	0.368 (0.288-0.448)	<0.001	6
CCTA Approach 0.50/5	422.3 ± 310.0	132.3 ± 143.3	0.99 (0.97-0.99)	<0.001	0.251 (0.195-0.308)	<0.001	2
Vessel volume (mm^3)							
NIRS-IVUS	963.8 ± 680.9						
CCTA Approach 0.75/1	614.8 ± 408.3	349.0 ± 296.4	0.98 (0.96-0.99)	<0.001	0.300 (0.249-0.352)	<0.001	3
CCTA Approach 0.75/2	621.5 ± 405.8	342.2 ± 319.2	0.98 (0.96-0.99)	<0.001	0.319 (0.264-0.375)	<0.001	4

	CCTA Approach 0.75/5	561.5 ± 376.4	402.3 ± 323.4	0.98 (0.97-0.99)	<0.001	0.279 (0.232-0.326)	<0.001	2
	CCTA Approach 0.50/1	613.7 ± 399.1	350.0 ± 322.4	0.98 (0.96-0.99)	<0.001	0.321 (0.260-0.381)	<0.001	5
	CCTA Approach 0.50/2	591.5 ± 391.3	372.2 ± 327.8	0.96 (0.94-0.98)	<0.001	0.376 (0.307-0.446)	<0.001	6
	CCTA Approach 0.50/5	577.9 ± 400.3	385.9 ± 295.8	0.99 (0.97-0.99)	<0.001	0.249 (0.199-0.298)	<0.001	1

Table footnote: ICC, intra-class correlation RC; repeatability coefficient

Note: Numbers in parentheses are 95% CIs.

*The rank is based on the combination of ICC and RC which were used to compare IVUS and CCTA algorithms. Lower rank indicates a better accuracy against IVUS estimations (rank 1 = best and rank 5 = worst)

Supplementary Table 3. Accuracy of CCTA reconstruction algorithms for detecting lesions using the NIRS-IVUS-based PB ≥ 40% cut-off and the cut-off derived from the ROC curve analysis

CT Reconstructions	Sensitivity (PB ≥ 40%)	Specificity (PB ≥ 40%)	New PB cut-off (%)*	Sensitivity (New PB)	Specificity (New PB)	Accuracy (New PB)
CCTA Approach 0.75/1	35%	94%	23.8	56%	80%	67%
CCTA Approach 0.75/2	35%	96%	30.5	47%	89%	67%
CCTA Approach 0.75/5	27%	98%	23.8	43%	89%	64%
CCTA Approach 0.50/1	36%	91%	28.2	54%	78%	65%
CCTA Approach 0.50/2	34%	93%	32.2	46%	85%	64%
CCTA Approach 0.50/5	29%	96%	27.4	43%	88%	64%

Table footnote: PB, plaque burden

*The new PB cut-off is refers to the best PB on each CCTA reconstructions that will detect a lesion derived from the ROC curve analysis

Supplementary Table 4. Accuracy of CCTA reconstruction algorithms for assessing lesion characteristics using the IVUS-derived PB cut-off of ≥ 40% over 3 consecutive frames.

NIRS-IVUS and CT reconstructions	Absolute estimations	Mean ± SD of differences	ICC	P	RC	P
Lesion length (mm)						
NIRS-IVUS	21.37 ± 19.12					
CCTA Approach 0.75/1	14.23 ± 12.40	10.66 ± 19.18	0.39 (0.15-0.59)	0.001	37.6 (29.1- 46.1)	<0.001
CCTA Approach 0.75/2	12.70 ± 13.78	11.20 ± 13.21	0.57 (0.37-0.72)	<0.001	25.9 (19.6-32.2)	<0.001
CCTA Approach 0.75/5	10.49 ± 13.22	16.50 ± 14.12	0.68 (0.49-0.81)	<0.001	27.7 (17.8-37.6)	<0.001
CCTA Approach 0.50/1	12.67 ± 13.19	10.80 ± 16.52	0.43 (0.20-0.61)	<0.001	32.4 (25.1-39.7)	<0.001
CCTA Approach 0.50/2	11.61 ± 11.52	12.18 ± 17.15	0.46 (0.24-0.63)	<0.001	33.6 (26.0-41.3)	<0.001
CCTA Approach 0.50/5	14.47 ± 17.18	10.03 ± 19.54	0.53 (0.31-0.71)	<0.001	38.3 (15.9-50.7)	<0.001
MLA (mm^2)						
NIRS-IVUS	4.64 ± 2.98					
CCTA Approach 0.75/1	2.88 ± 1.92	1.11 ± 1.82	0.62 (0.42-0.76)	<0.001	1.27 (1.00-1.53)	<0.001

CCTA Approach 0.75/2	3.49 ± 2.95	0.59 ± 2.03	0.59 (0.39-0.84)	<0.001	1.48 (0.85-2.12)	<0.001
CCTA Approach 0.75/5	2.58 ± 2.03	0.78 ± 1.23	0.52 (0.27-0.71)	<0.001	1.65 (1.10-2.19)	<0.001
CCTA Approach 0.50/1	2.99 ± 2.18	1.59 ± 2.41	0.55 (0.35-0.70)	<0.001	1.49 (0.99-1.98)	<0.001
CCTA Approach 0.50/2	2.71 ± 1.87	1.76 ± 2.65	0.53 (0.33-0.69)	<0.001	1.85 (0.94-1.83)	<0.001
CCTA Approach 0.50/5	2.84 ± 2.34	1.09 ± 2.71	0.54 (0.31-0.71)	<0.001	1.87 (1.09-2.65)	<0.001
PB (%)						
NIRS-IVUS	63.9 ± 13.2					
CCTA Approach 0.75/1	66.9 ± 15.3	-0.005 ± 15.67	0.41 (0.17-0.61)	0.001	30.7 (24.6-36.8)	<0.001
CCTA Approach 0.75/2	63.7 ± 15.5	3.19 ± 13.51	0.56 (0.35-0.72)	<0.001	26.5 (21.7-31.3)	<0.001
CCTA Approach 0.75/5	66.7 ± 17.3	3.53 ± 15.19	0.51 (0.25-0.70)	<0.001	29.8 (25.2-34.3)	<0.001
CCTA Approach 0.50/1	66.5 ± 15.2	-1.43 ± 15.27	0.43 (0.21-0.61)	<0.001	29.9 (16.0-33.8)	<0.001
CCTA Approach 0.50/2	67.3 ± 14.9	-1.75 ± 15.07	0.44 (0.22-0.62)	<0.001	29.5 (25.4-33.7)	<0.001
CCTA Approach 0.50/5	64.6 ± 15.6	2.97 ± 14.32	0.53 (0.30-0.70)	<0.001	28.1 (23.9-32.2)	<0.001
Remodeling Index						
NIRS-IVUS	0.81 ± 0.22					
CCTA Approach 0.75/1	0.94 ± 0.29	-0.12 ± 0.30	0.37 (0.09-0.60)	0.006	0.60 (0.42-0.77)	<0.001
CCTA Approach 0.75/2	0.95 ± 0.34	-0.17 ± 0.33	0.26 (0.00-0.51)	0.04	0.65 (0.49-0.81)	<0.001

CCTA Approach 0.75/5	0.93 ± 0.32	-0.14 ± 0.33	0.26 (0.00-0.54)	0.06	0.65 (0.46-0.84)	<0.001
CCTA Approach 0.50/1	0.91 ± 0.29	-0.12 ± 0.32	0.26 (0.00-0.49)	0.03	0.63 (0.47-0.79)	<0.001
CCTA Approach 0.50/2	0.92 ± 0.30	-0.12 ± 0.32	0.33 (0.06-0.56)	0.008	0.62 (0.47-0.78)	<0.001
CCTA Approach 0.50/5	0.94 ± 0.59	-0.14 ± 0.52	0.37 (0.00-0.66)	0.03	1.02 (0.54-1.51)	<0.001

Table footnote: ICC, intra-class correlation coefficient; MLA, minimum lumen area; PB, plaque burden; SD, standard deviation; RC, repeatability coefficient

Note: Numbers in parentheses are 95% CIs.

*Numbers in parentheses are 95% CIs.

Supplementary Table 5. Comparison of the lumen, vessel and plaque area and PB estimations differences between IVUS and CCTA reconstruction algorithms at a cross-sectional-level.

NIRS-IVUS and CT reconstructions	Absolute estimations	Mean ± SD of differences	ICC	P	Overall rank
Mean Lumen area (mm^2)					
NIRS-IVUS	8.45 ± 5.13				
CCTA Approach 0.75/1	6.61 ± 4.02	1.84 ± 1.71	0.84 (0.84-0.85)	<0.001	1
CCTA Approach 0.75/2	6.73 ± 3.91	1.72 ± 1.77	0.83 (0.82-0.84)	<0.001	4
CCTA Approach 0.75/5	6.41 ± 3.98	2.04 ± 1.71	0.83 (0.83-0.84)	<0.001	3
CCTA Approach 0.50/1	6.42 ± 3.72	2.02 ± 1.96	0.80 (0.79-0.80)	<0.001	5
CCTA Approach 0.50/2	6.32 ± 3.73	2.13 ± 2.01	0.79 (0.78-0.80)	<0.001	6
CCTA Approach 0.50/5	6.43 ± 3.91	2.02 ± 1.74	0.84 (0.83-0.84)	<0.001	2
Mean Vessel area (mm^2)					
NIRS-IVUS	14.58 ± 7.44				
CCTA Approach 0.75/1	9.30 ± 5.07	5.28 ± 3.12	0.85 (0.85-0.86)	<0.001	3
CCTA Approach 0.75/2	9.45 ± 5.14	5.13 ± 3.18	0.84 (0.84-0.85)	<0.001	4

CCTA Approach 0.75/5	8.58 ± 4.88	6.00 ± 3.11	0.85 (0.85-0.86)	<0.001	2
CCTA Approach 0.50/1	9.30 ± 4.93	5.28 ± 3.20	0.83 (0.82-0.83)	<0.001	5
CCTA Approach 0.50/2	9.03 ± 4.87	5.55 ± 3.32	0.82 (0.82-0.83)	<0.00	6
CCTA Approach 0.50/5	9.79 ± 5.05	5.78 ± 2.94	0.88 (0.88-0.89)	<0.001	1
Plaque area (mm^2)					
NIRS-IVUS	6.13 ± 3.51				
CCTA Approach 0.75/1	2.69 ± 2.47	3.44 ± 2.34	0.62 (0.61-0.64)	<0.001	2
CCTA Approach 0.75/2	2.72 ± 2.65	3.42 ± 2.34	0.62 (0.61-0.64)	<0.001	3
CCTA Approach 0.75/5	2.17 ± 2.12	3.96 ± 2.34	0.60 (0.58-0.61)	<0.001	6
CCTA Approach 0.50/1	2.87 ± 2.63	3.26 ± 2.30	0.62 (0.60-0.63)	<0.001	4
CCTA Approach 0.50/2	2.72 ± 2.54	3.41 ± 2.28	0.60 (0.59-0.62)	<0.001	5
CCTA Approach 0.50/5	2.37 ± 2.40	3.76 ± 2.21	0.68 (0.66-0.69)	<0.001	1
PB (%)					
NIRS_IVUS	41.85 ± 14.92				
CCTA Approach 0.75/1	27.95 ± 17.37	13.90 ± 12.30	0.55 (0.53-0.56)	<0.001	2
CCTA Approach 0.75/2	27.33 ± 16.92	14.51 ± 11.97	0.56 (0.54-0.57)	<0.001	1
CCTA Approach 0.75/5	24.63 ± 16.30	17.22 ± 12.25	0.52 (0.50-0.54)	<0.001	4

CCTA Approach 0.50/1	29.29 ± 17.49	12.56 ± 12.89	0.50 (0.48-0.52)	<0.001	5
CCTA Approach 0.50/2	28.68 ± 17.12	13.17 ± 12.67	0.50 (0.48-0.51)	<0.001	6
CCTA Approach 0.50/5	25.63 ± 16.31	16.22 ± 12.26	0.53 (0.51-0.54)	<0.001	3

Table footnote: ICC, intraclass correlation coefficient; SD, standard deviation

Note: Numbers in parentheses are 95% CIs.

*****Lower rank indicates a better accuracy against IVUS estimations (rank 1 = best and rank 5 = worst).

Supplementary Table 6. Intra- and inter-observer reproducibility analysis.

Metrics	Mean ± SD of differences	ICC	Correlation Coefficient
Intra-observer analysis			
Lumen area (mm^2)	0.77 ± 0.98	0.97 (0.96 - 0.97)	0.94
Vessel area (mm^2)	0.89 ± 1.08	0.97 (0.97 - 0.97)	0.94
Plaque area (mm^2)	0.92 ± 1.21	0.87 (0.85 - 0.89)	0.74
Plaque burden (%)	7.97 ± 8.35	0.85 (0.82 - 0.87)	0.79
Inter-observer analysis			
Lumen area (mm^2)	1.03 ± 1.35	0.96 (0.95 - 0.97)	0.94
Vessel area (mm^2)	1.47 ± 1.90	0.94 (0.91 - 0.96)	0.90
Plaque area (mm^2)	1.08 ± 1.31	0.82 (0.81 - 0.84)	0.72
Plaque burden (%)	8.53 ± 8.32	0.84 (0.82 - 0.85)	0.71

Table footnote: ICC, intra-class correlation coefficient; SD, standard deviation

Note: Numbers in parentheses are 95% CIs.

Figures

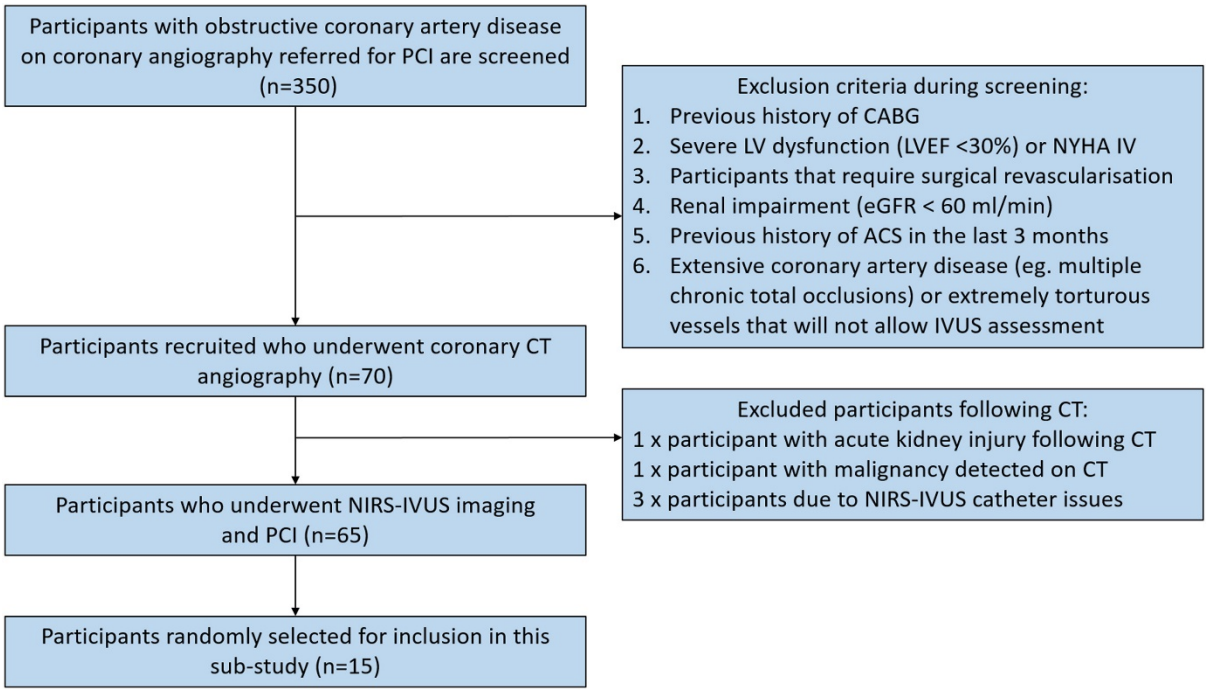

Figure 1. Study flowchart.

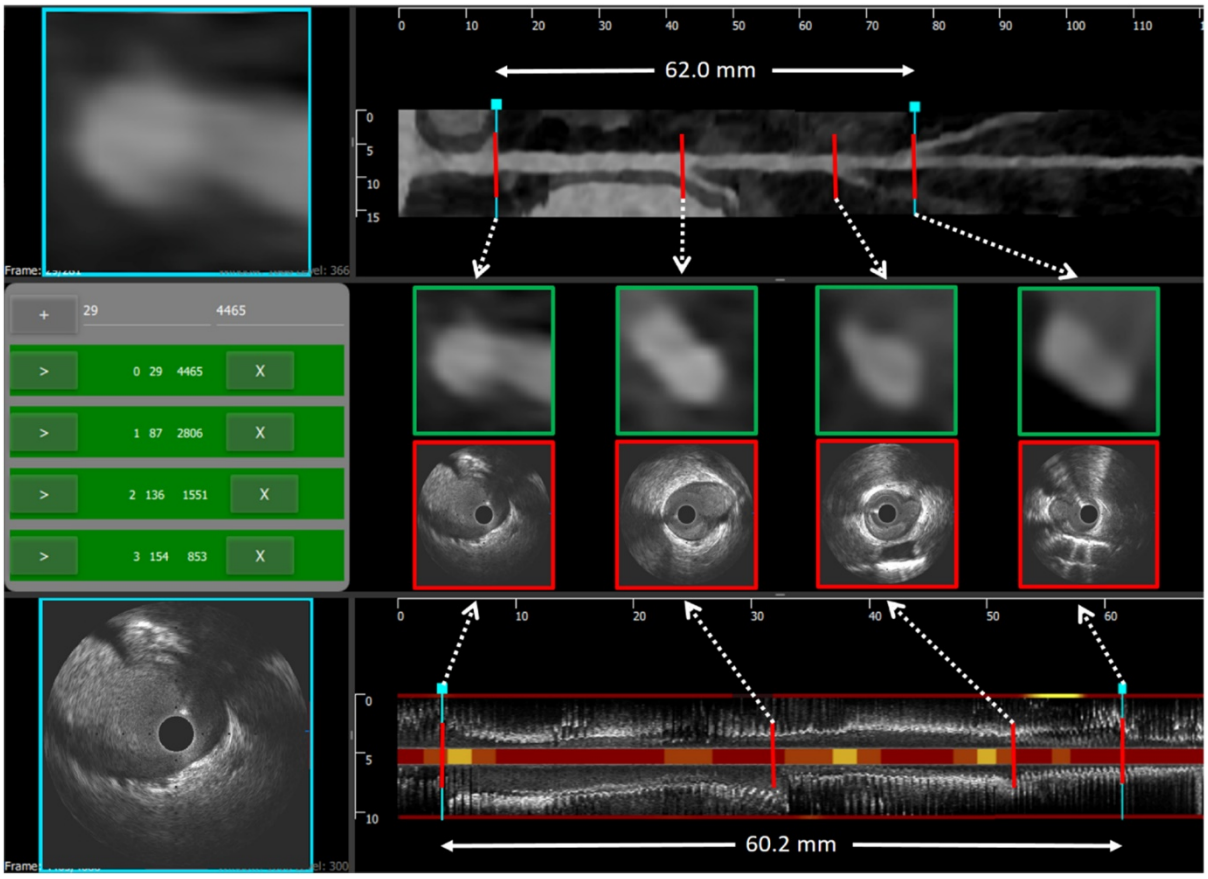

Figure 2. Snapshot of the software for the co-registration of the IVUS and CCTA images. A longitudinal view of the IVUS pullback along with the annotated end-diastolic NIRS-IVUS frames are seen on the top panel (green) while the bottom panel shows the segment of interest in CCTA and corresponding cross-sectional images (red). The CCTA images are mapped onto the IVUS images along its centerline; anatomical landmarks such as side branches are identified on both modalities and used to identify corresponding frames/cross-section; the CCTA frames in between landmarks are interpolated. The software allows the corrected slice-by-slice comparison between IVUS and CCTA.

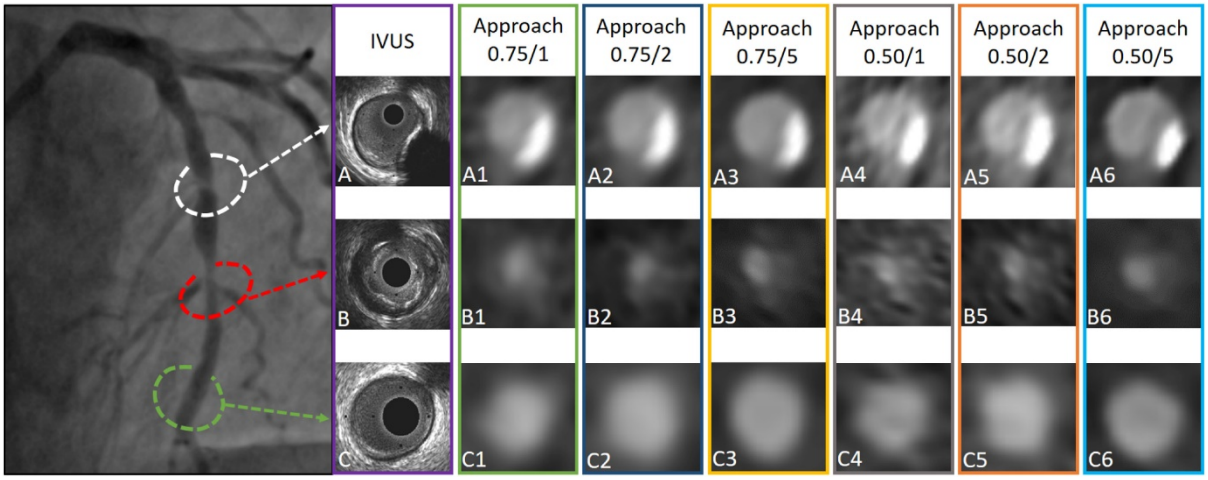

Figure 3. Case examples highlighting the effects of slice thickness and IR strengths on plaque visualization in CCTA. In all causes CCTA reconstruction was performed using the medium smooth b40f kernel. On the top panel, there is a calcified plaque in the mid vessel of a left anterior descending artery (white dotted circle) with the corresponding IVUS (A) and CCTA reconstruction (Panel A1 to A6). In the middle panel, there is a large non-calcified plaque as seen on the coronary angiography (red dotted circle). The corresponding IVUS frame (B) and CCTA reconstruction (Panel B1 to B6) are shown in panels B and B1-6 respectively. The bottom panel shows a relatively normal vessel (green dotted circle) with corresponding IVUS (C) and CCTA reconstruction (Panel C1 to C6).

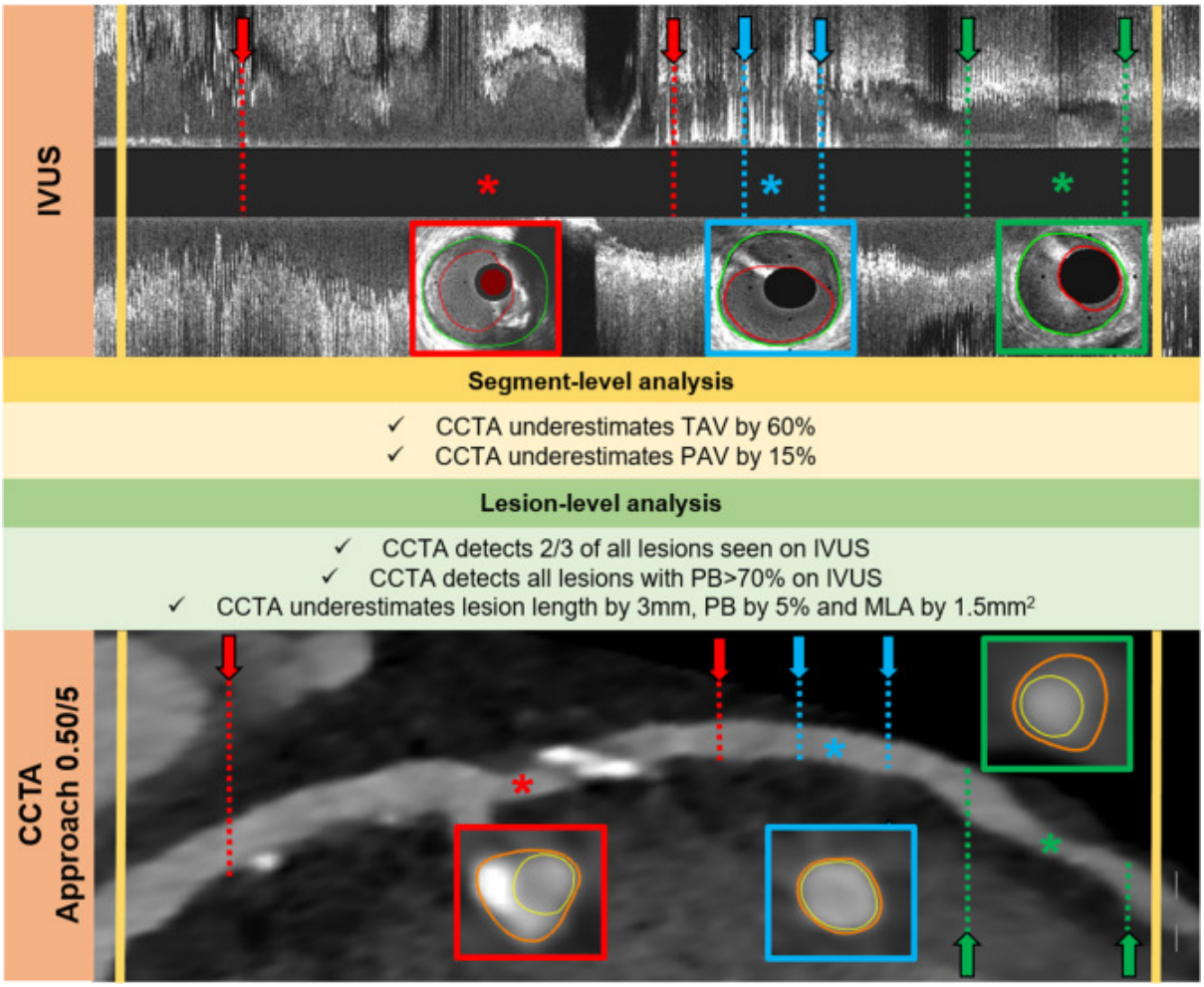

Figure 4. IVUS and corresponding CCTA longitudinal and cross-sectional images reconstructed using the 0.50/5 approach. Overall CCTA considerably underestimates the PAV and TAV for the segment of interest (marked with a yellow vertical line in both modalities) and is capable to detect only 2 out of the 3 lesions detected on IVUS (the proximal and distal reference site of each lesion is located with vertical lines while the * indicate the location of the MLA shown in the IVUS and coronary CTCA cross-sectional images). CT angiography detected the calcified plaque (red square) and a large fibrotic plaque (green square) but missed the fibrotic plaque with smaller PB (blue square) compared to IVUS. CCTA underestimates lesion length, PB and MLA compared with IVUS.

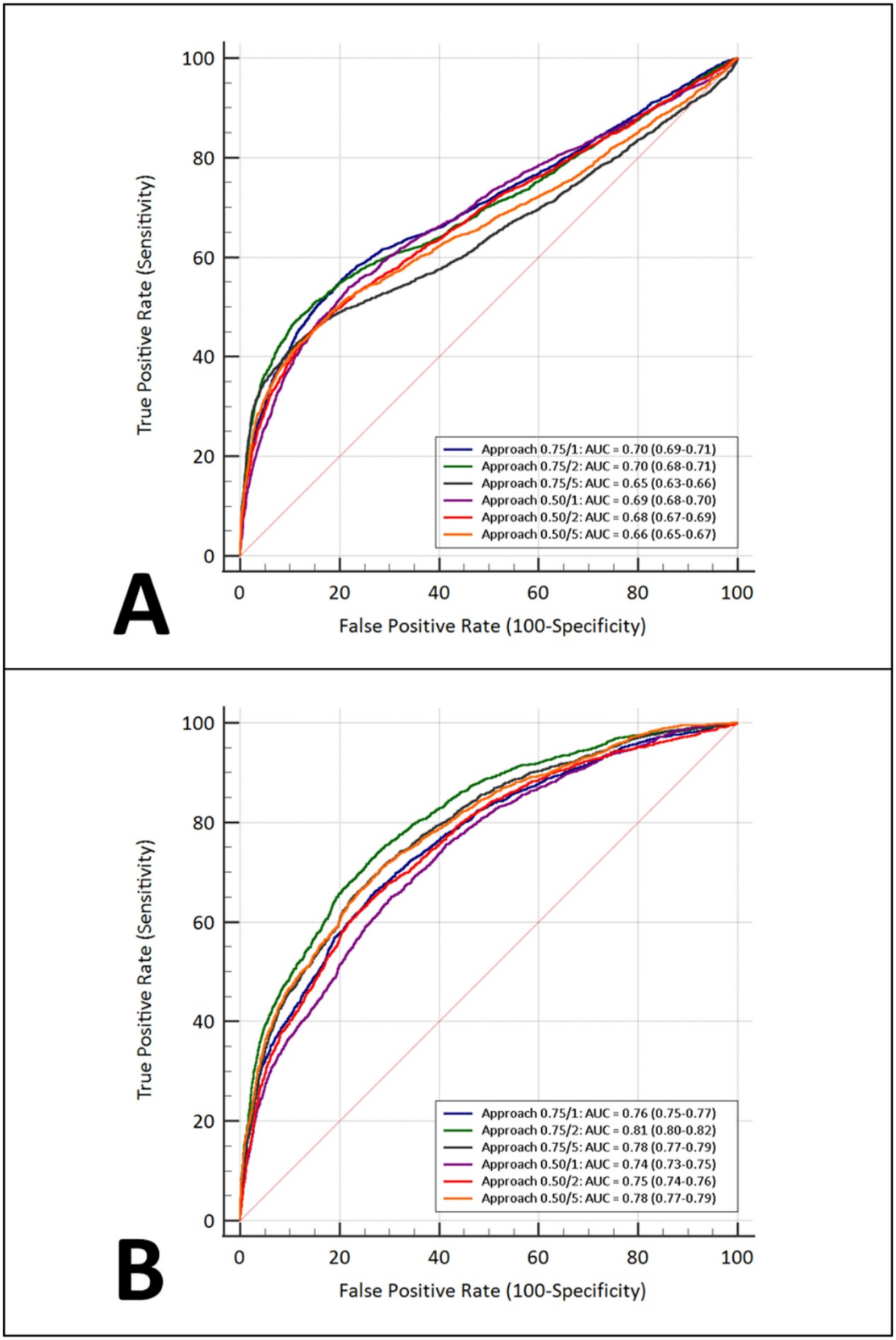

Figure 5. Efficacy of the 6 CCTA reconstruction algorithms for detecting lesions using a PB cut-off of 40% (A) and using the best cut-off estimated for each approach (B).

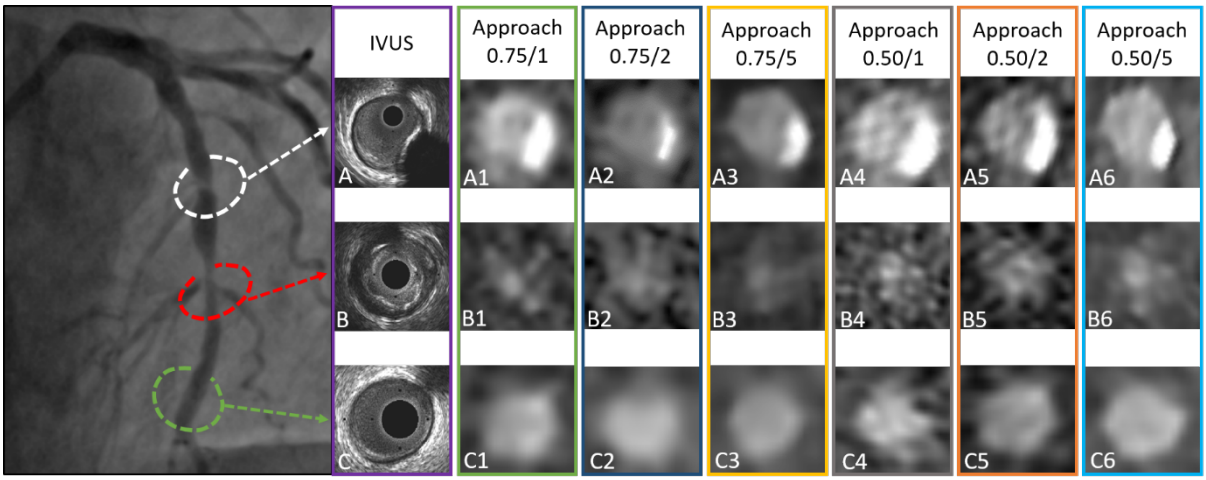

Supplementary Figure 1. Case examples showing the poor image quality of the CCTA reconstructions obtained using the sharp b49f kernel. The studied vessel has discrete lesions a coronary angiographic image is shown in left panel. On the top panel, there is a calcified plaque in the mid vessel of a left anterior descending artery (white dotted circle) with the corresponding IVUS (A) and CCTA reconstruction (Panel A1 to A6). In the middle panel, there is a large non-calcified plaque as seen on the coronary angiography (red dotted circle). The corresponding IVUS frame (B) and CCTA reconstruction (Panel B1 to B6) are shown in panels B and B1-6 respectively. The bottom panel shows a relatively normal vessel (green dotted circle) with corresponding IVUS (C) and CCTA reconstruction (Panel C1 to C6).

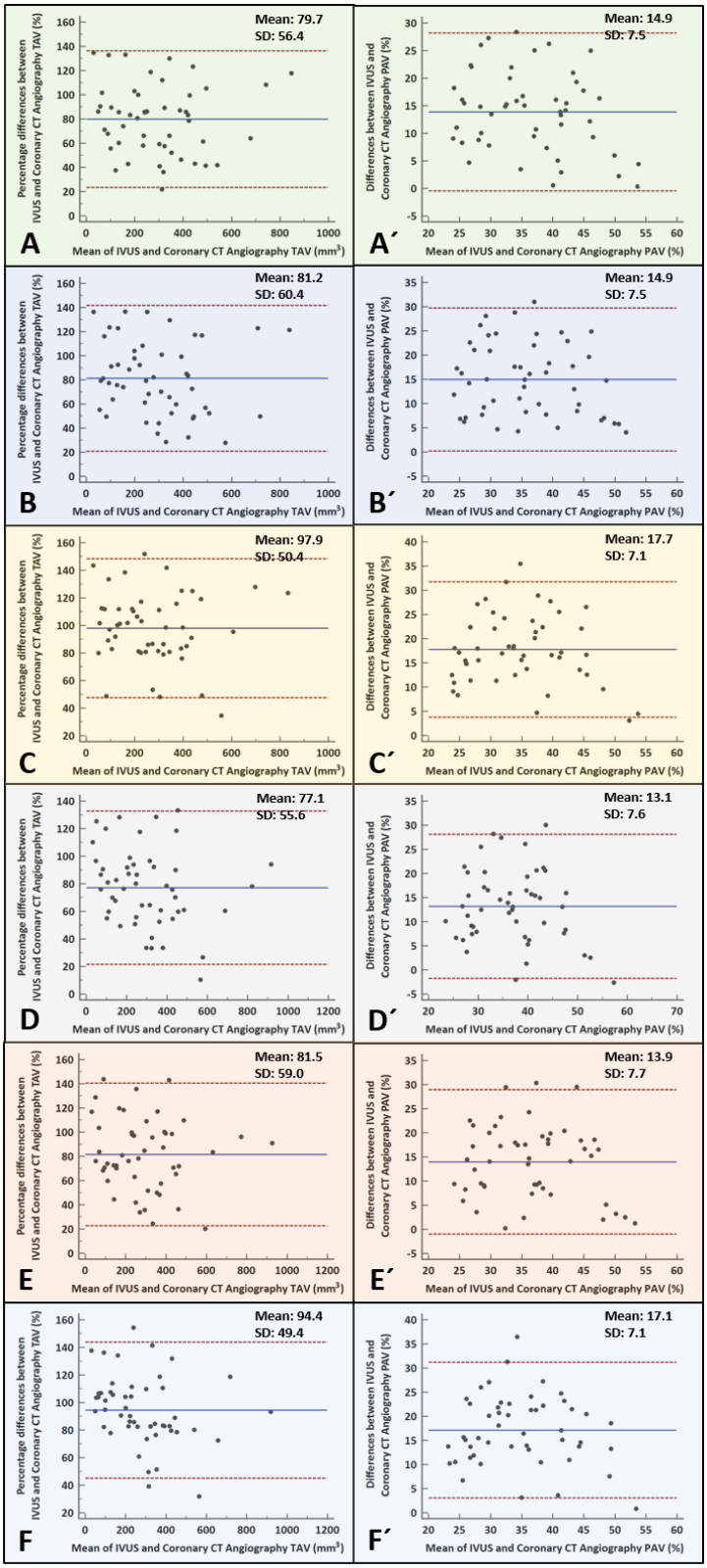

Supplementary Figure 2. Bland-Altman plots of the percentage mean differences between IVUS and coronary CTA reconstruction approaches for TAV (A: 0.75/1, B: 0.75/2, C: 0.75/5, D: 0.50/1, E: 0.50/2, F: 0.50/5) and PAV (A´: 0.75/1, B´: 0.75/2, C´: 0.75/5, D´: 0.50/1, E´: 0.50/2, F´: 0.50/5).

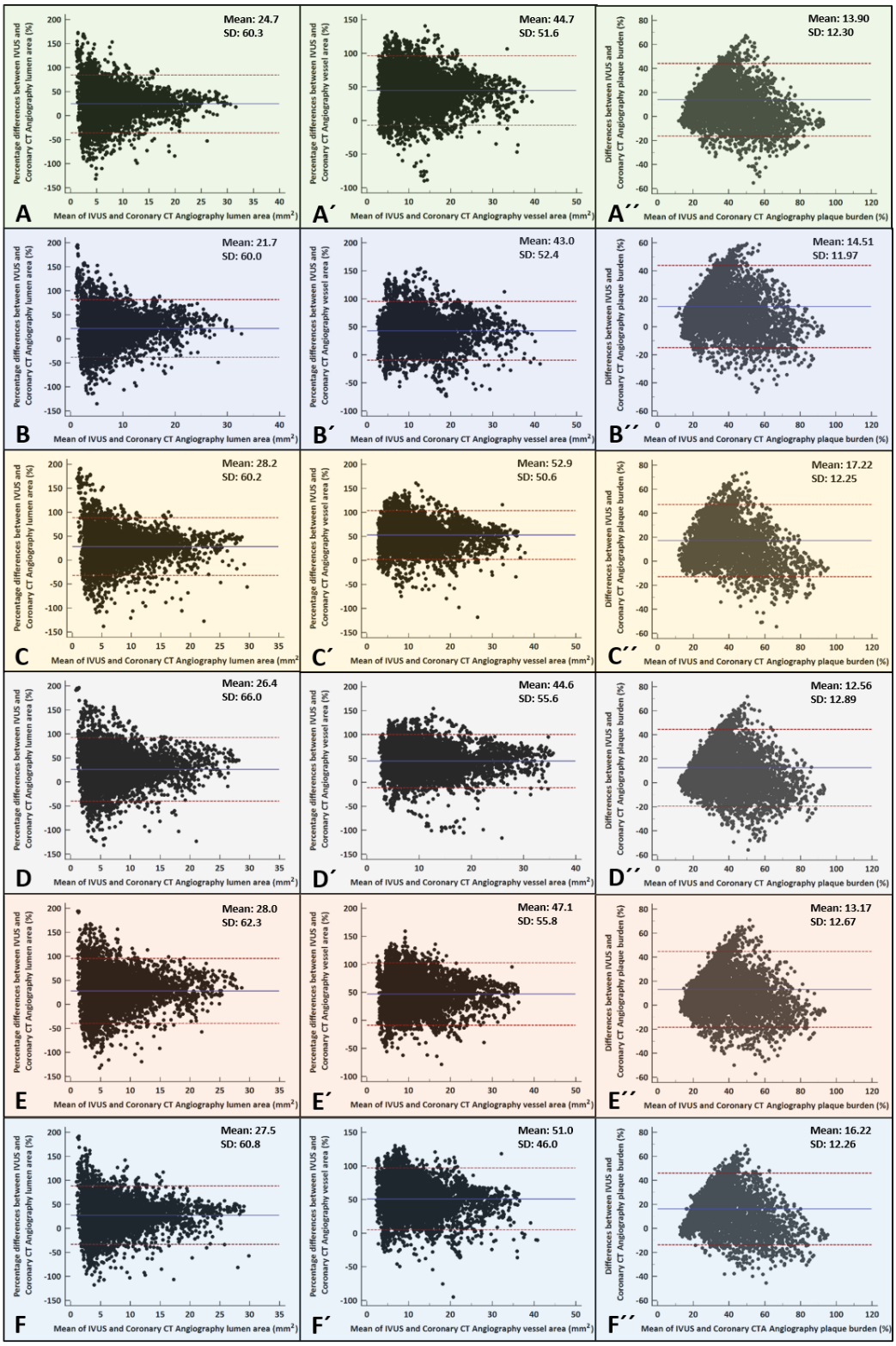

Supplementary Figure 3. Bland-Altman analysis of the percentage mean differences between IVUS and CCTA approaches for cross-sectional level lumen area (A: 0.75/1, B: 0.75/2, C: 0.75/5, D: 0.50/1, E: 0.50/2 and F: 0.50/5), vessel area (A´: 0.75/1, B´: 0.75/2, C´: 0.75/5, D´: 0.50/1, E´: 0.50/2, F´: 0.50/5) and PB (A´´: 0.75/1, B´´: 0.75/2, C´´: 0.75/5, D´´: 0.50/1, E´´: 0.50/2 and F´´: 0.50/5.

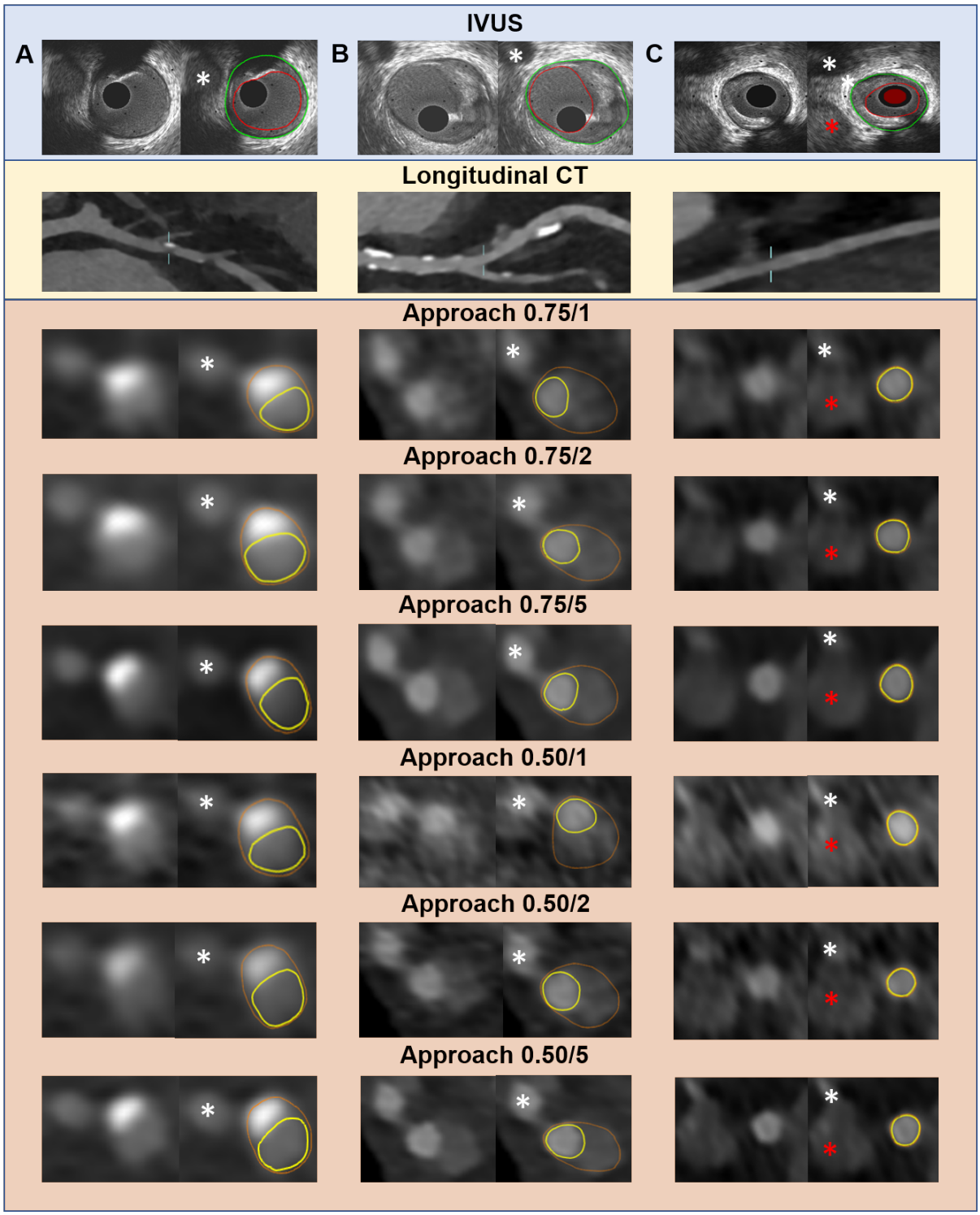

Supplementary Figure 4. Case examples highlighting the limitations of CCTA in assessing PB using IVUS as the reference standard. CCTA images with and without contour overlay are shown. From these images, it is apparent that higher strength IR reconstruction approach allows better visualization of the plaque. Panel A, portrays a calcific plaque seen in the mid left anterior descending artery (LAD) on IVUS. The longitudinal view of the vessel on CCTA (reconstructed using approach 0.5/5) and the

corresponding cross-sections reconstructed using the 6 CCTA reconstruction approaches are also displayed. The diagonal side branch seen on both modalities that indicates correspondence is marked with a white asterisk. The blooming artefact on CCTA resulted in significant overestimation of the plaque area (range: 5.5 – 6.7mm^2) and PB (range: 47.8 – 59.8%) on CCTA images compared to the IVUS (plaque area: 5.1mm^2 and PB: 40.8%). In the middle panel (Panel B), there is a non-calcific plaque in the mid LAD; the diagonal branch indicating correspondence is marked with a white asterisk on both modalities. The PB on CCTA images (range in different reconstruction approaches: 69.7 – 75.1% is overestimated by >20% compared to the corresponding IVUS cross-section (PB: 47.5%). On the right panel (Panel C), there is a fibrotic plaque (PB: 49.8%) seen on the IVUS image in the mid circumflex artery; an obtuse marginal branch marked with white asterisk and cardiac vein with red asterisk were used to identify matching. The corresponding CCTA cross-sections reconstructed using the tested approaches are also displayed. It is apparent that CCTA failed to detect the presence of a plaque in this segment.